

**Supplementary Information for “Comparison of BARRA and ERA5 in replicating mean and extreme precipitation over Australia” by Cheung et al.**

Table S1 Summary of literature review in Section 1

<b>Study</b>	<b>Reanalysis Datasets</b>	<b>Variables</b>	<b>Major Findings</b>
Quagraine et al. (2020)	ERA-Interim, ERA5, JRA-55, MERRA2, NCEP-R2	Precipitation	All represent monsoon rainfall pattern and seasonal cycle well over west Africa
Dai et al. (2023)	ERA5	Precipitation	Rainfall erosivity over Loess Plateau consistent with station data
Cheung et al. (2023)	ERA5	Convective parameters	Applied to evaluate RCM simulations
Betts et al. (2019)	ERA-Interim, ERA5	Precipitation	Biases in ERA5 over Canadian Prairies smaller
Hu and Yuan (2021) and Jiang et al. (2021)	ERA5	Precipitation	Overall spatiotemporal patterns in Eastern Tibet Plateau captured, but under- (over-) estimated rain intensity (duration)
Jiao et al. (2021)	ERA5	Precipitation	High spatiotemporal correlation with observation in China, but over-estimated summer rainfall
Izadi et al. (2021)	ERA5	Precipitation	Monthly/seasonal rainfall matches with observation better than daily data in Iran
Qin et al. (2021)	ERA5	Precipitation	Over- (under-) estimated rain frequency (intensity) in China
Lei et al. (2022) and Shen et al. (2022)	ERA5	Extreme climate indices	Moderate extremes better estimated than high-end extremes
Wang et al. (2019)	ERA-Interim, ERA5	Surface temperature, precipitation, snow	Warm biases over Arctic Sea, ERA5 has thinner ice thickness
Lei et al. (2020)	ERA-Interim, ERA5	Cloud cover	ERA5 much better than ERA-Interim over east China but not Tibet Plateau
Gleixner et al. (2020)	ERA-Interim, ERA5	Temperature, precipitation	Biases smaller and interannual variability improved over East Africa
Song and Wei (2021)	ERA5, MERRA-2	Precipitation	Both have reasonable diurnal cycle over north China, ERA5 has better afternoon peak
Li et al. (2022)	ERA-Interim, ERA5, JRA55, MERRA	Precipitation	ERA5 generally better than the other over the Poyang Lake Basin, China
May et al. (2021)	BARRA	Surface variables	High correlations with station data over Northern Australia

Pirooz et al. (2021)	ERA-Interim, ERA5, ERA5-land, BARRA	Winds, precipitation, temperature	BARRA better than the ERA's for precipitation and temperature, good gust wind speed but ERA5 the best in gust frequency
Du et al. (2023)	BARRA	Precipitation	Climatology for ungauged catchments in Australia
Hobeichi et al. (2023)	BARRA, BARRA-C	Various	Applied to train statistical downscaling models
Su et al. (2019)	BARRA, ERA-Interim, MERRA-2	Surface temperature and pressure, winds, precipitation	Smaller biases over Australia in BARRA compared with the other two
Acharya et al. (2019, 2020)	BARRA	Precipitation	Daily / sub-daily rain better over temperate Australia than tropical region
Nishant et al. (2022)	BARRA, BARRA-C	Precipitation	High-resolution BARRA-C only better in specific locations
Choudhury et al. (2023)	ERA5	Extreme temperature	Mean temperature better than the extremes
<b>This study</b>	<b>BARRA, ERA5</b>	<b>Precipitation, climate extreme indices</b>	<b>Section 6</b>

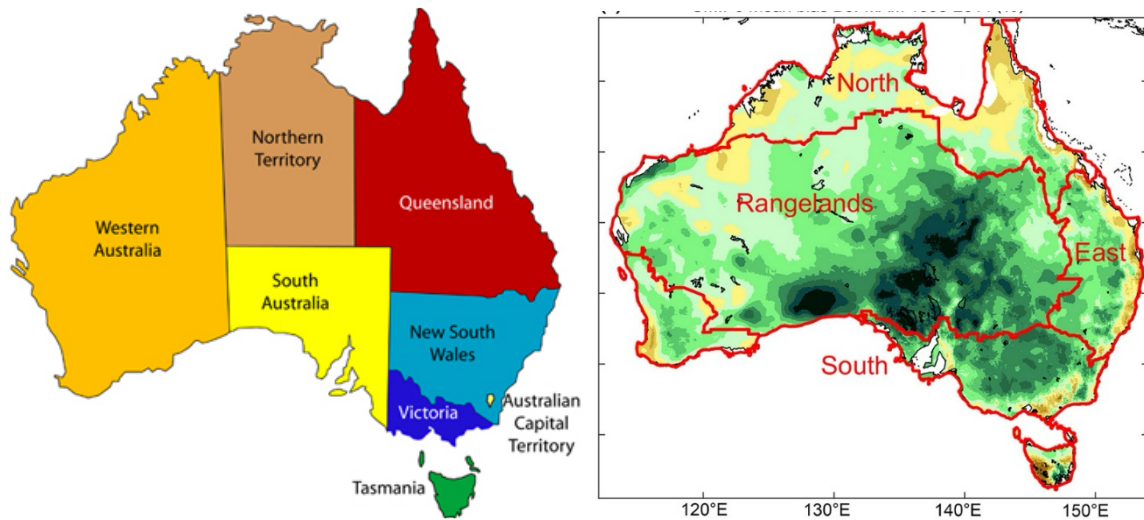


Figure S 1 Australia map with states and territories (left) with borders of the four “supercluster” averaging regions (right): Northern Australia (North), Rangelands, Southern Australia (South), Eastern Australia (East) and topography.

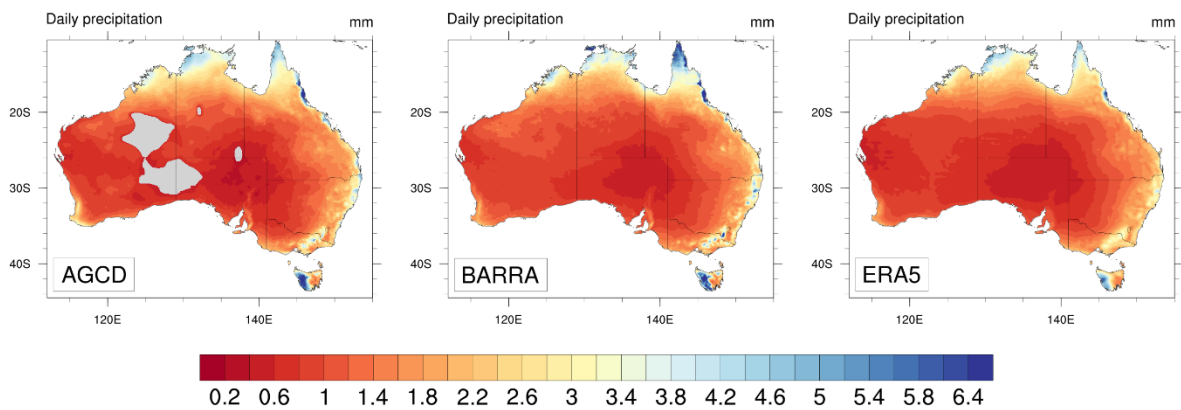


Figure S 2 Annual mean precipitation of AGCD, BARRA and ERA5 on AGCD grids.

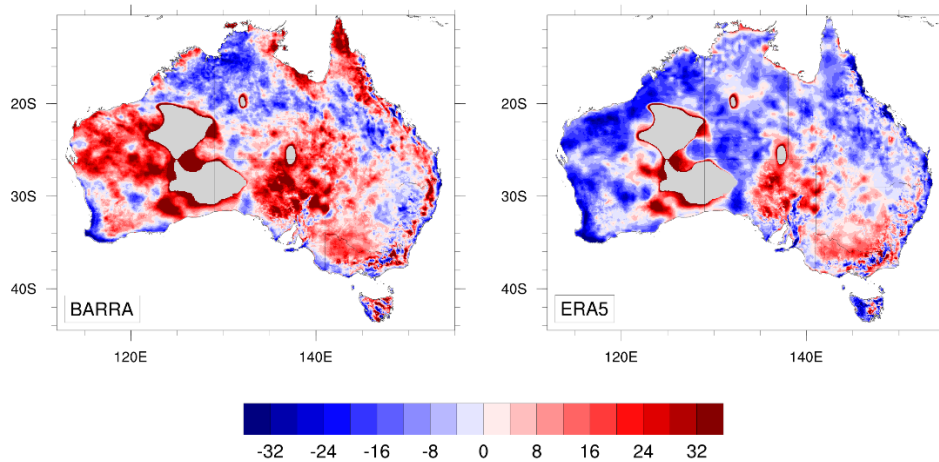


Figure S 3 Relative bias (%) of precipitation in BARRA and ERA5 evaluated at 5-km resolution (AGCD grids).

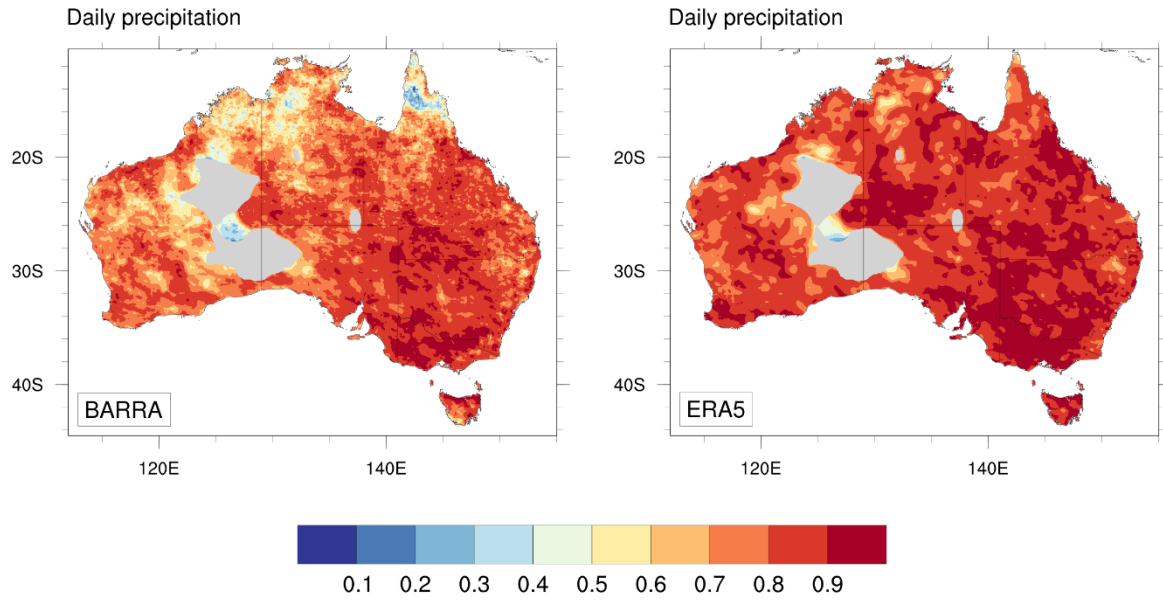


Figure S 4 Temporal correlation coefficient of annual precipitation between BARRA/ERA5 and AGCD on AGCD grids.

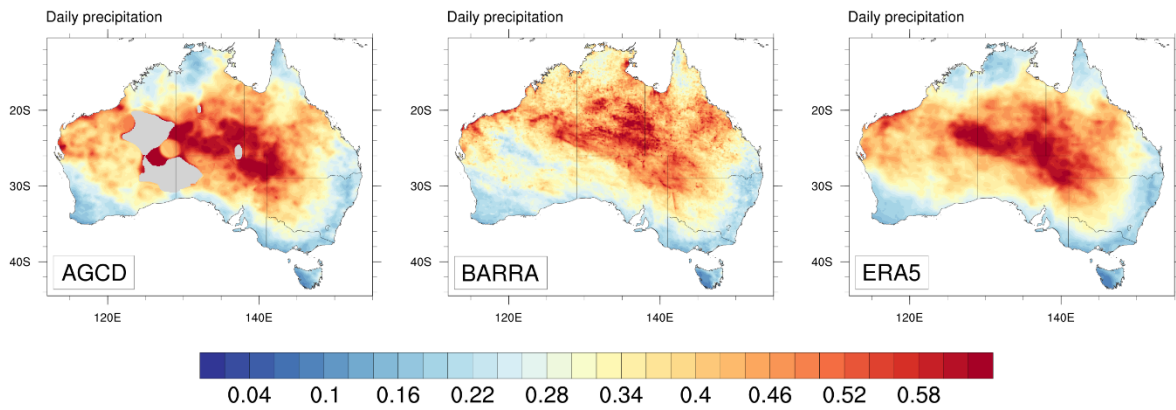


Figure S 5 CV of annual precipitation for AGCD, BARRA and ERA5 on AGCD grids.

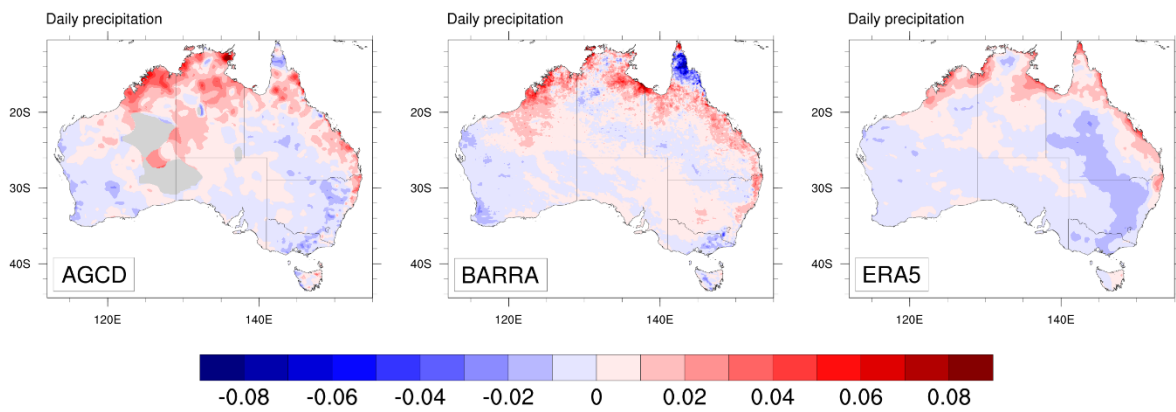


Figure S 6 Trend of annual precipitation for AGCD, BARRA and ERA5 on AGCD grids.

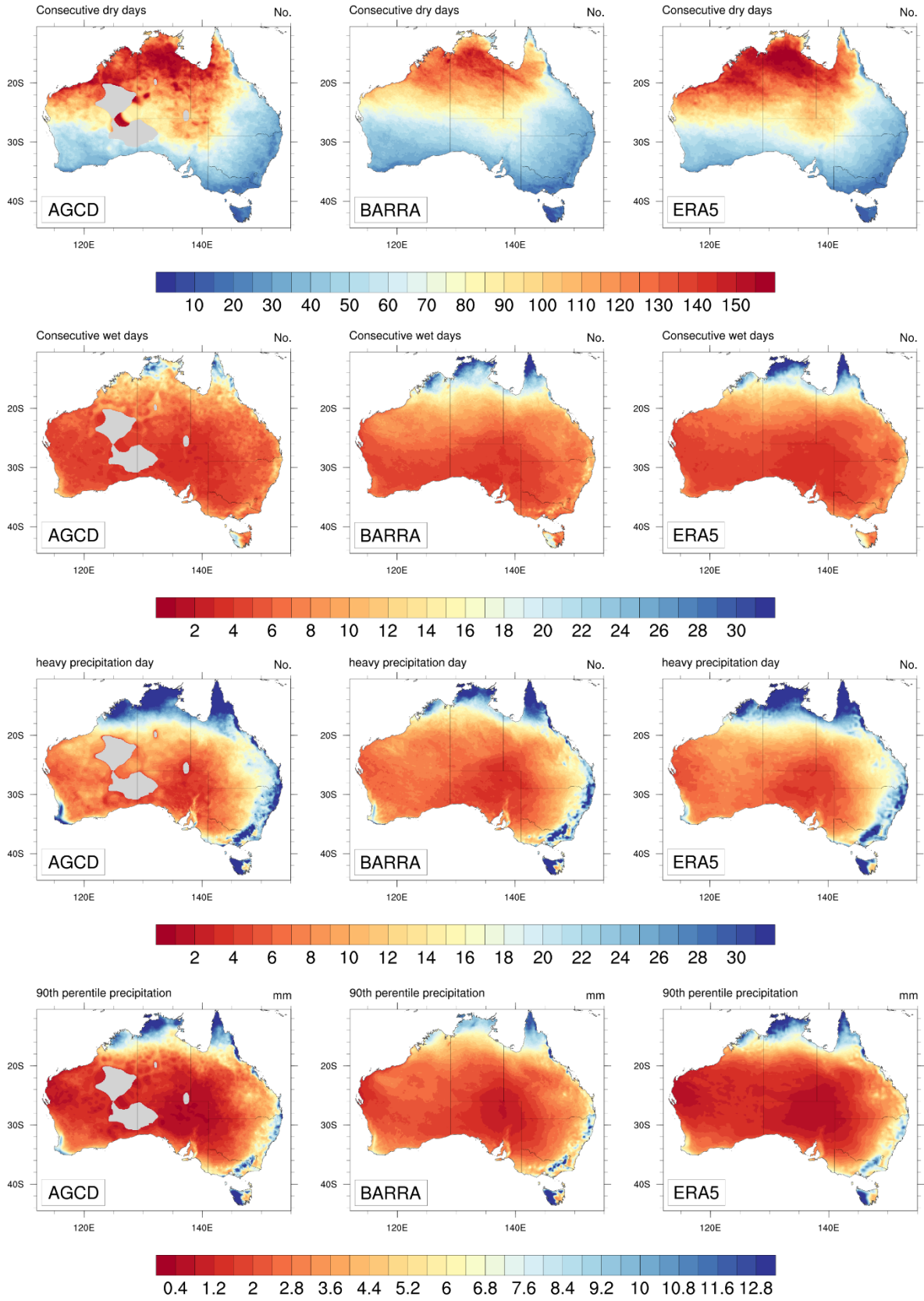


Figure S 7 Mean CDD, CWD, R10mm, R90p, R99p and Rx1day of AGCD, BARRA and ERA5 on AGCD grids.

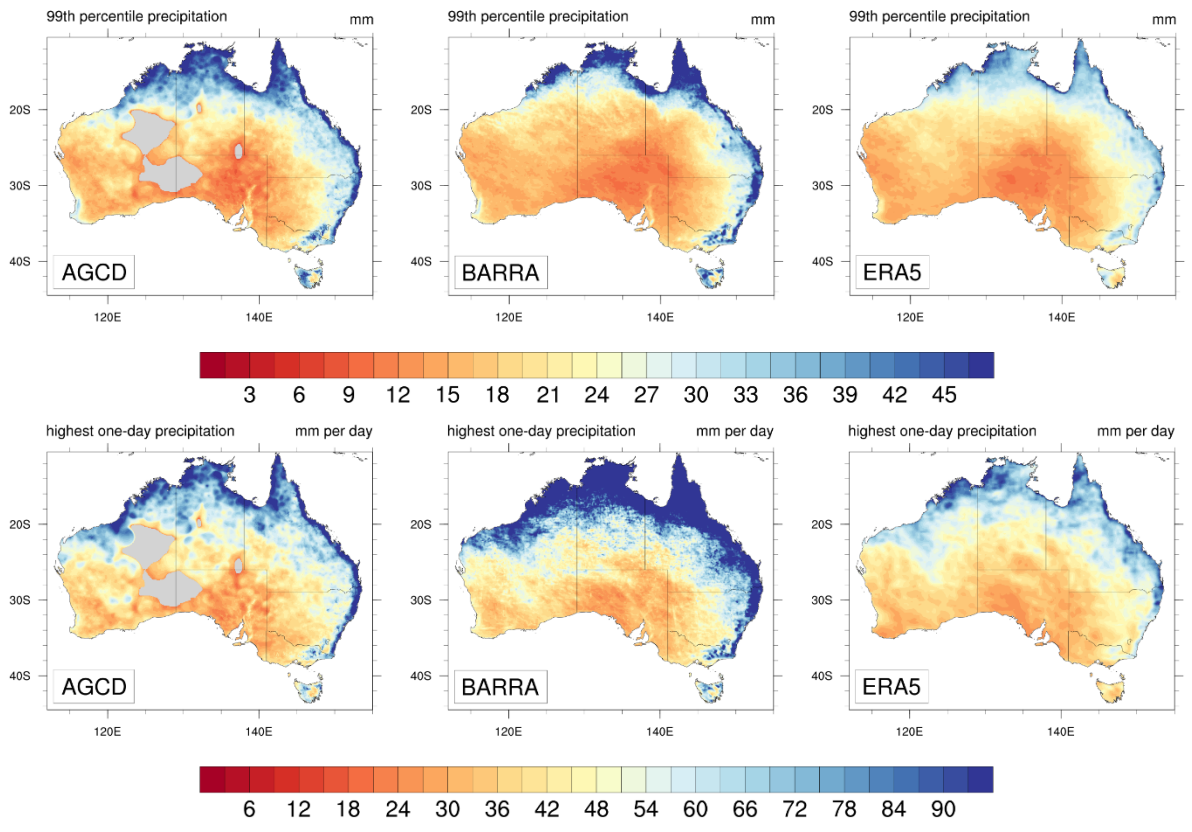


Figure S 7 (continued).

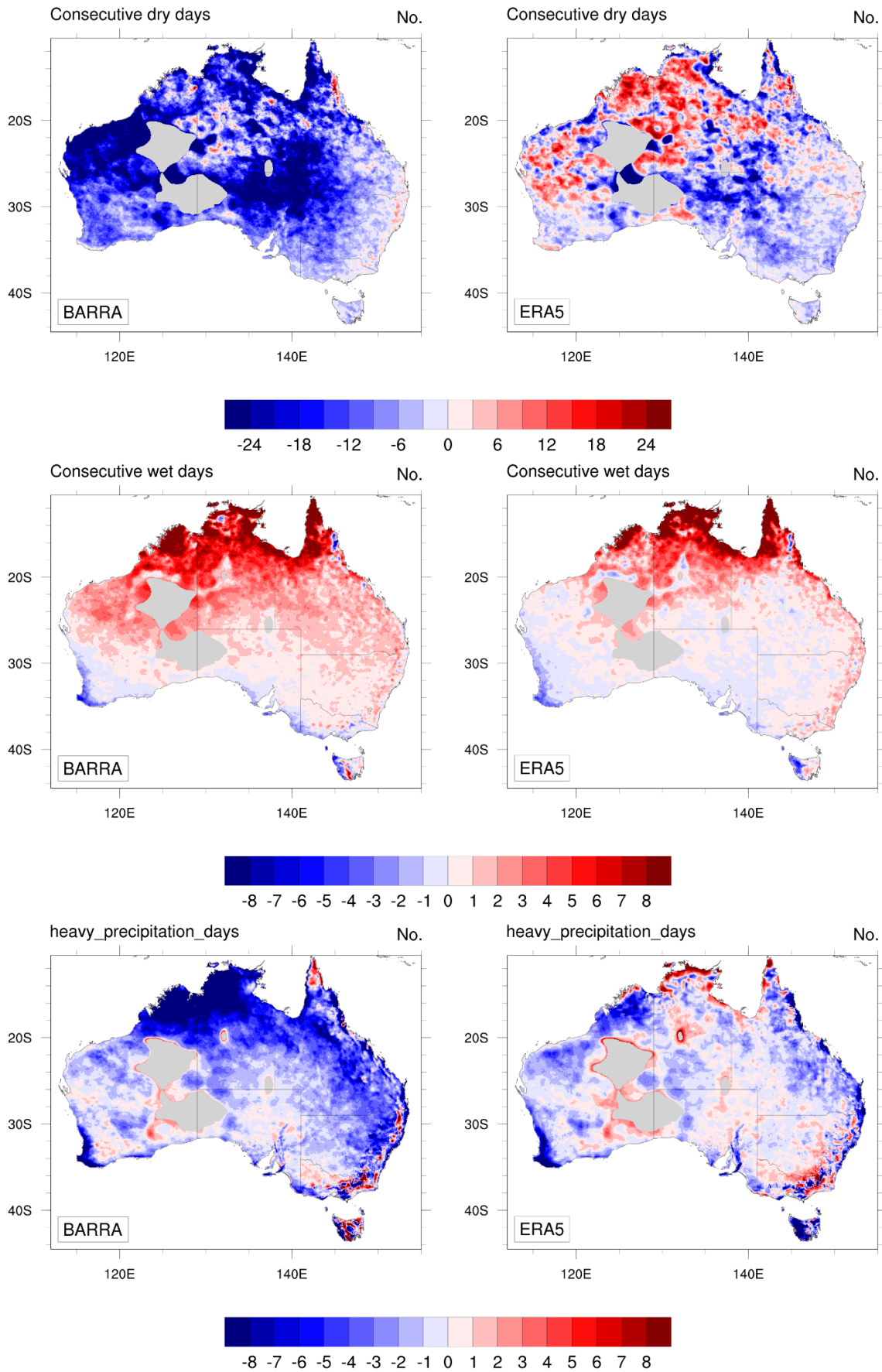


Figure S 8 Biases in CDD, CWD, R10mm, R90p, R99p and Rx1Day in BARRA (left column) and ERA5 (right column) on AGCD grids.

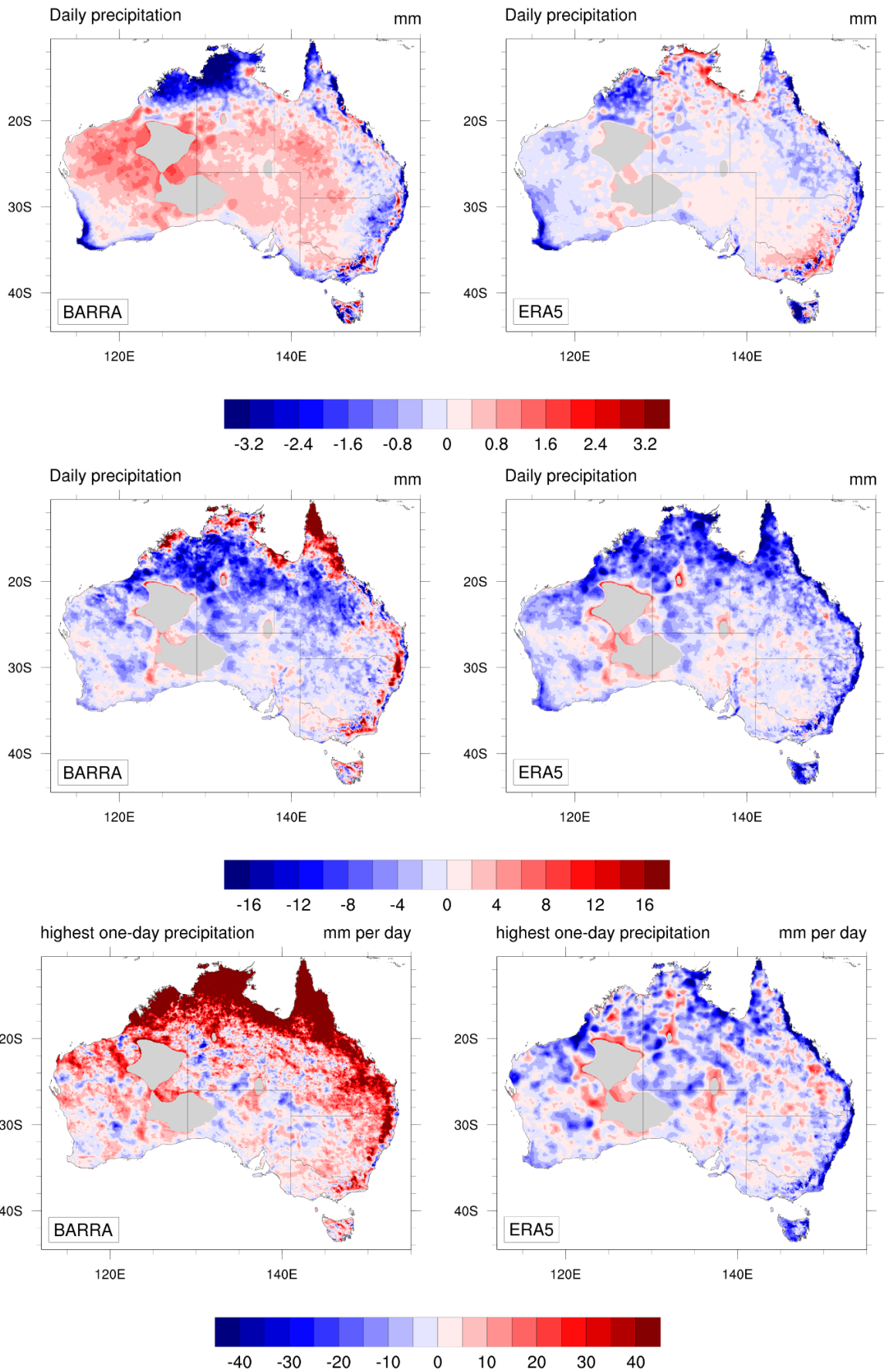


Figure S 8 (continued).



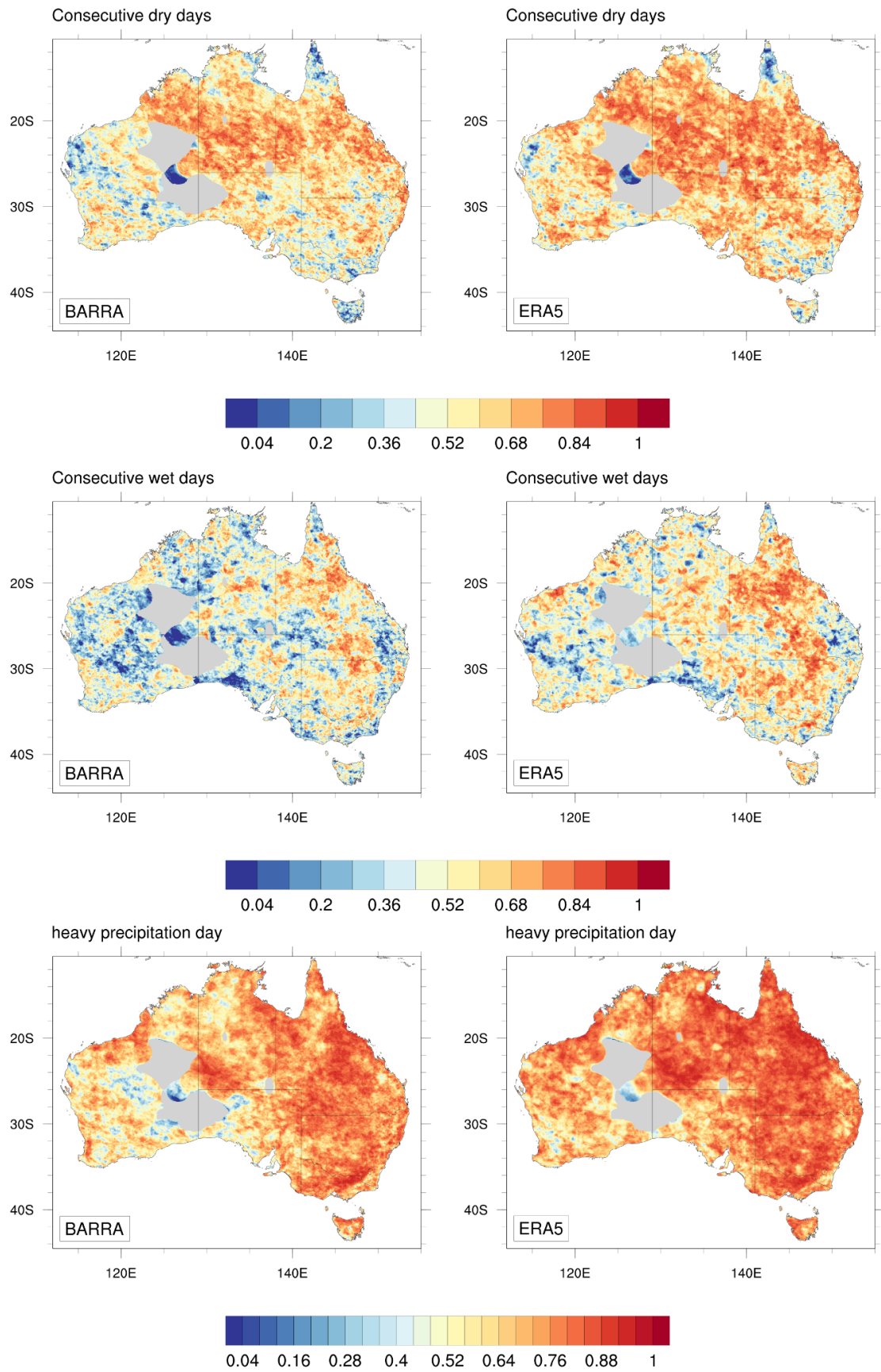


Figure S 9 Temporal correlation of CDD, CWD, R10mm, R90p, R99p and Rx1Day between BARRA and AGCD (left column) and between ERA5 and AGCD (right column) on AGCD grids.

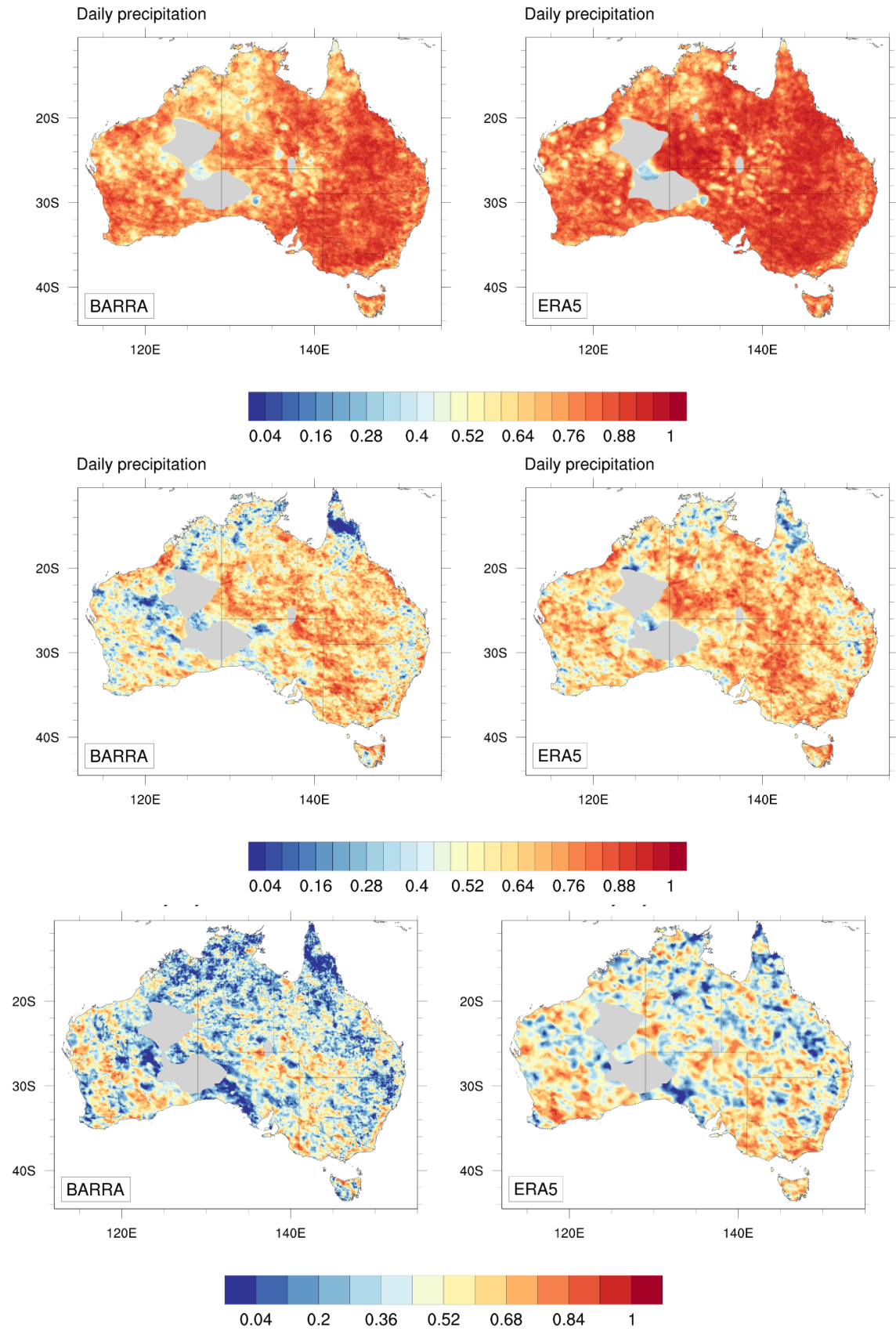


Figure S 9 (continued).

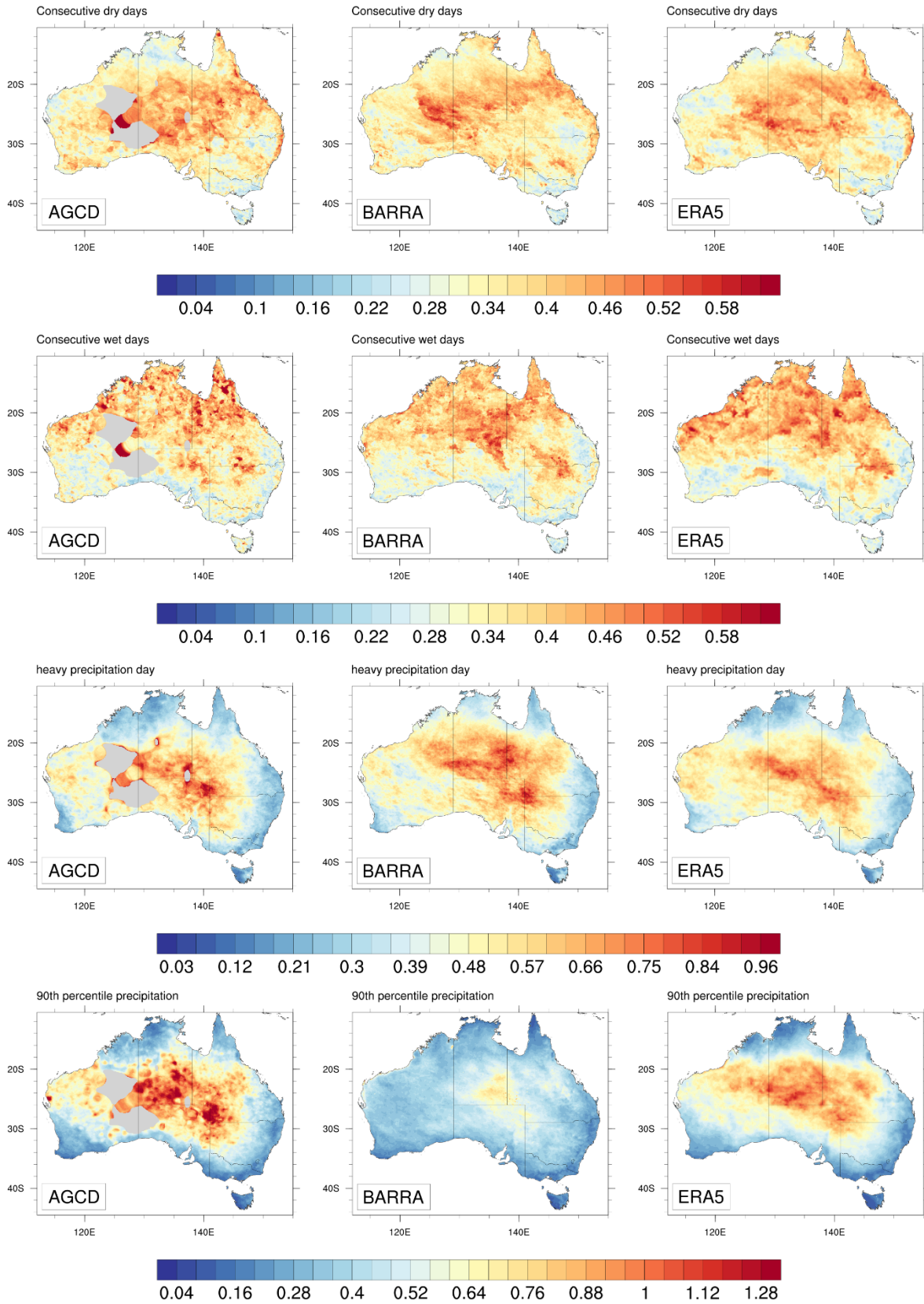


Figure S 10 CV of annual precipitation, CDD, CWD, R10mm, R90p, R99p and Rx1day for AGCD, BARRA and ERA5, on AGCD grids.

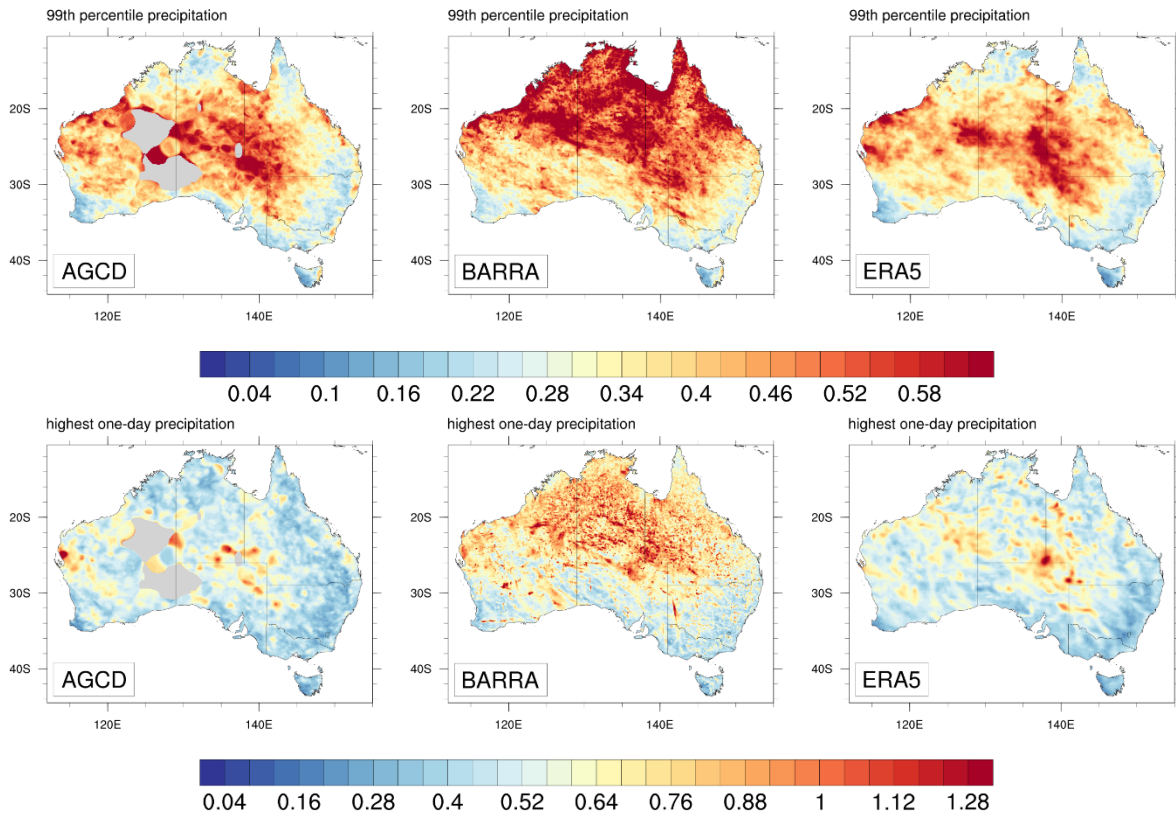


Figure S 10 (continued).

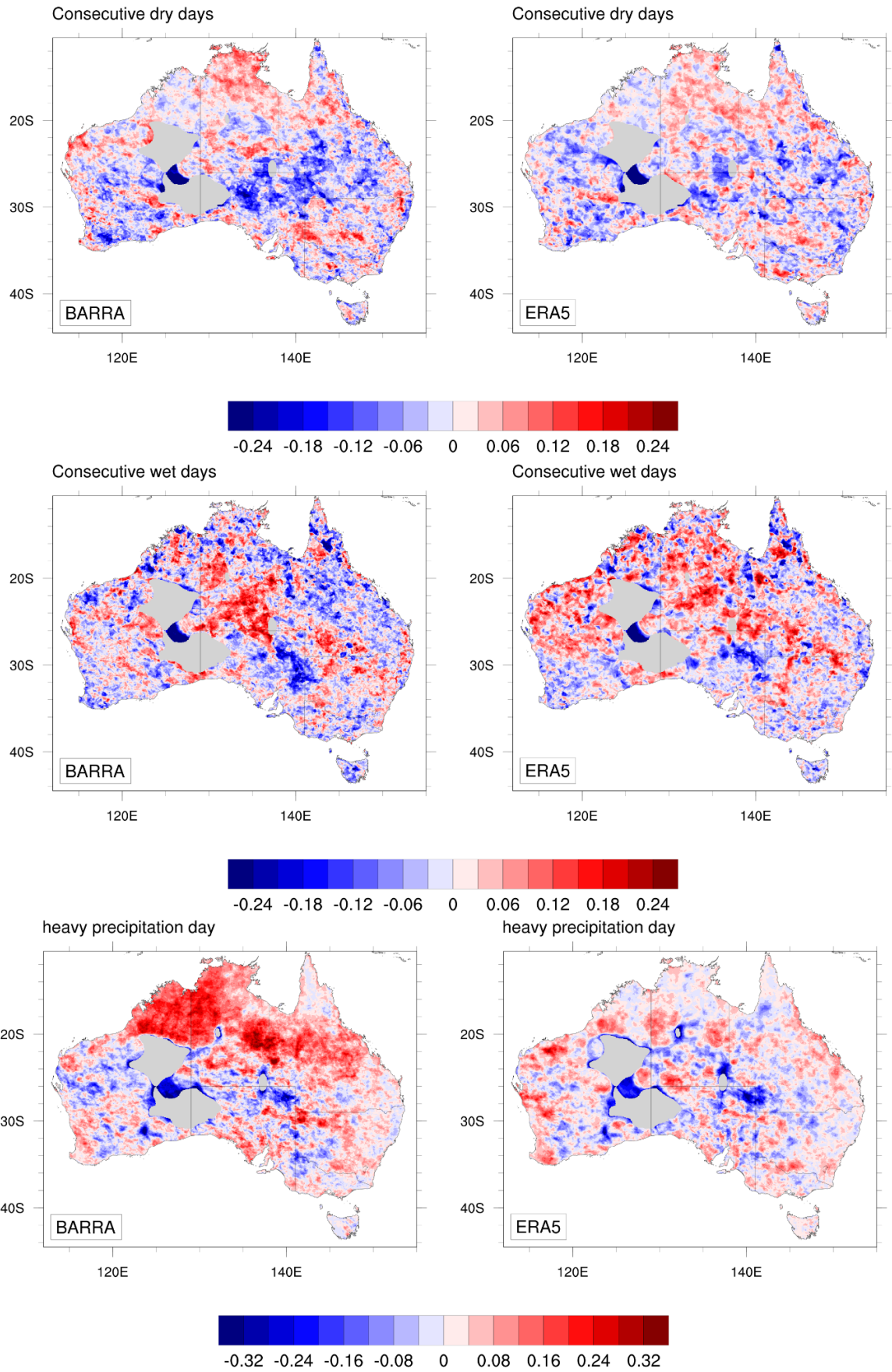


Figure S 11 Biases in CV of CDD, CWD, R10mm, R90p, R99p and Rx1Day for BARRA (left column) and ERA5 (right column) relative to AGCD, on AGCD grids.

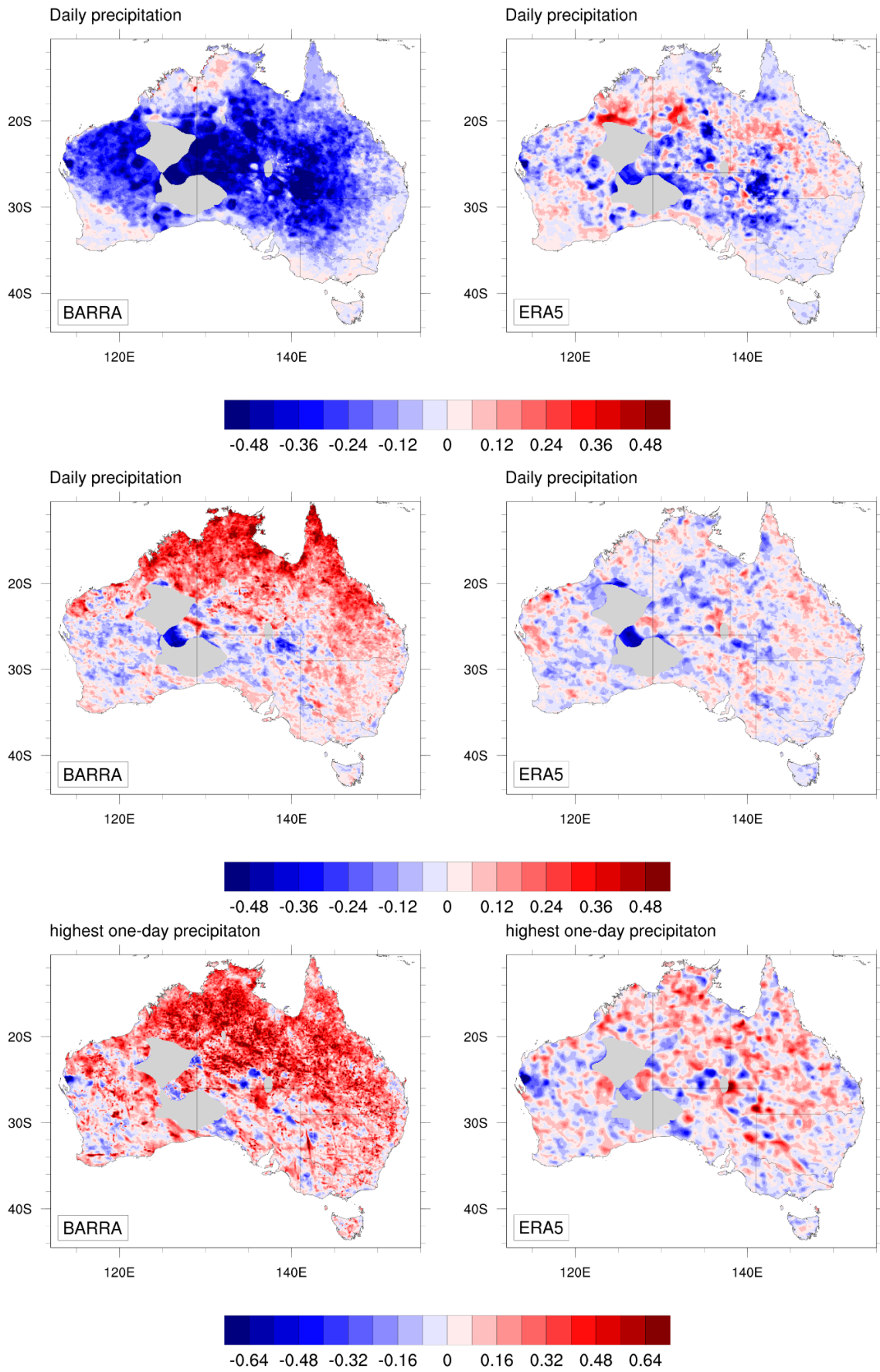


Figure S 11 (continued).

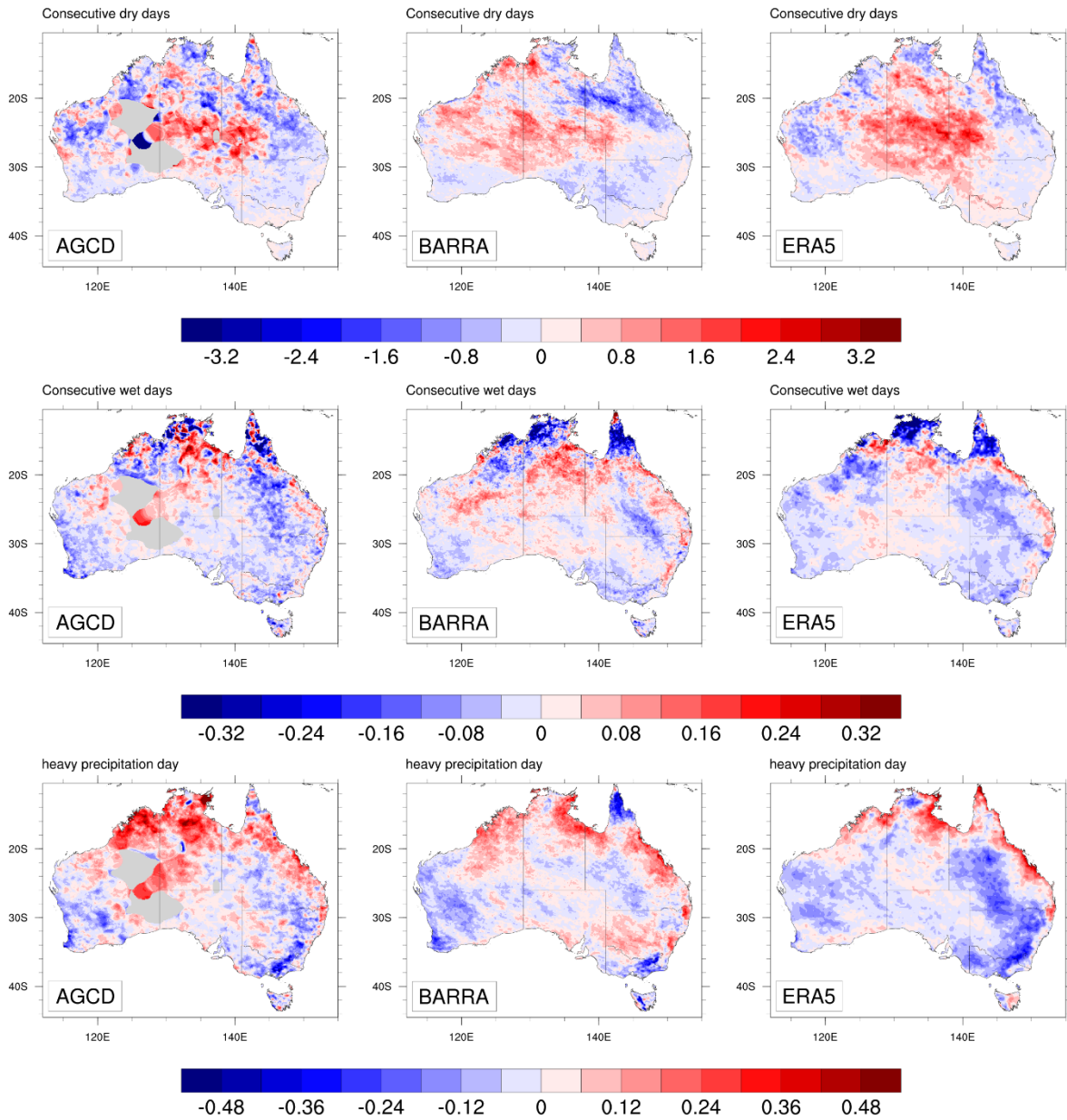


Figure S 12 Trend of annual precipitation, CDD, CWD, R10mm, R90p, R99p and Rx1day for AGCD, BARRA and ERA5, on AGCD grids.

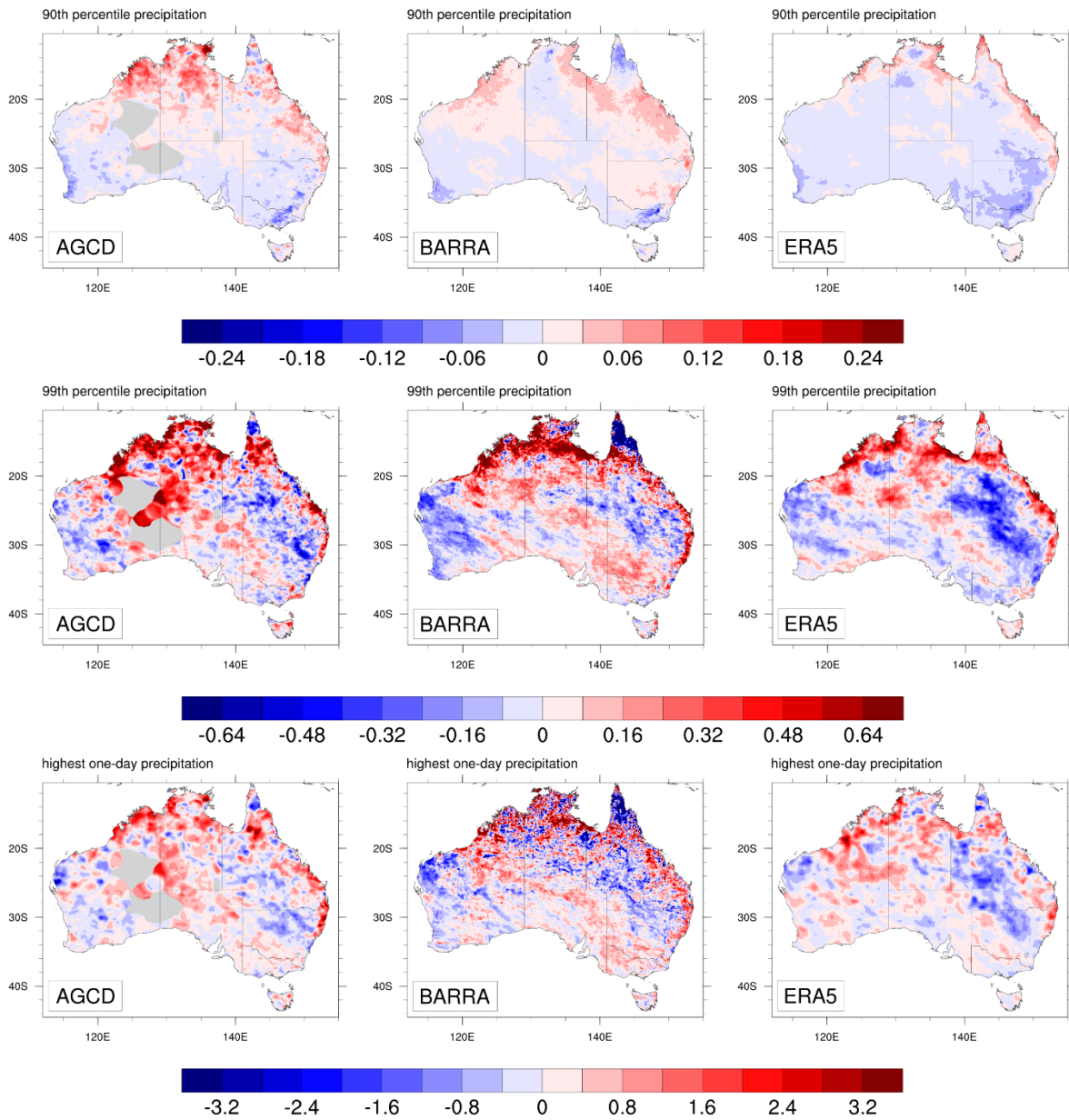


Figure S 12 (continued).



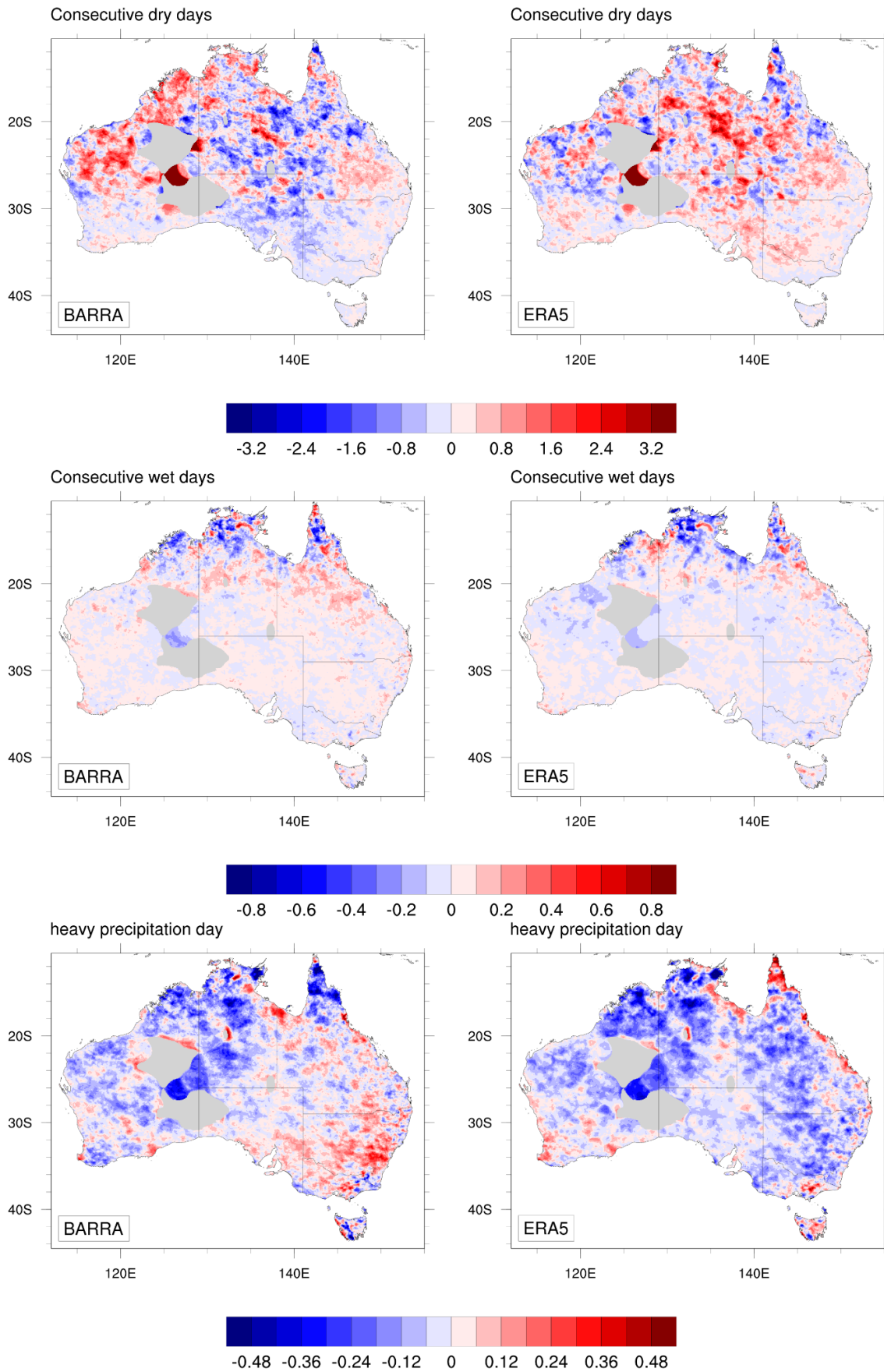


Figure S 13 Biases in trends of CDD, CWD, R10mm, R90p, R99p and Rx1Day for BARRA (left column) and ERA5 (right column) relative to AGCD, on AGCD grids.

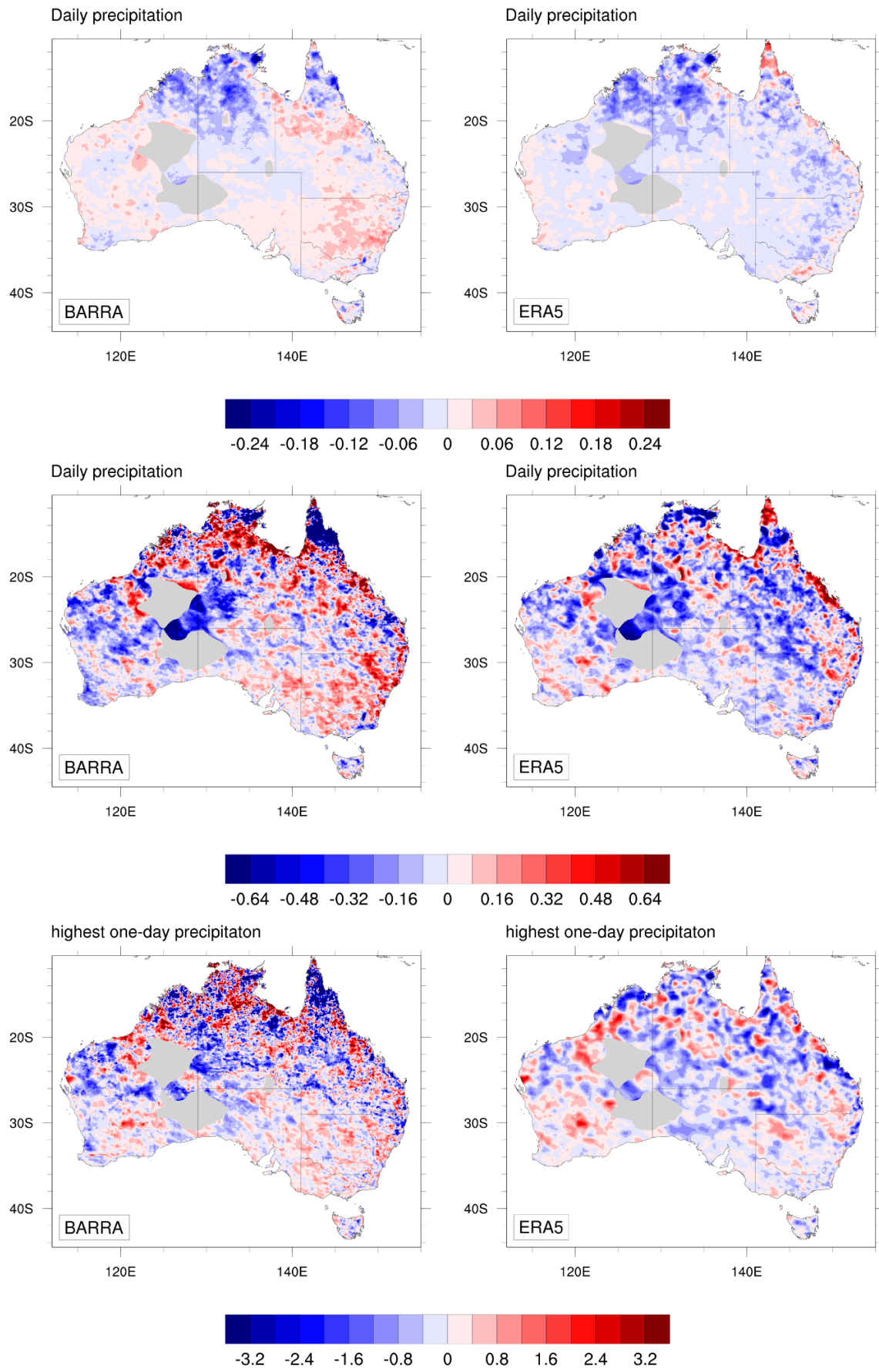


Figure S 13 (continued).